

Indoleacetic acid-mediated suppression of oxidation and crystallization in tin perovskite LEDs

Lei Wang^{a,b}, Bing Han^a, Yu Lou^c, Haoran Wang^{c*}, Chengjian Chen^{a*} and Yang Bai^{b,c}

^a College of Materials Science and Engineering, Hunan University, Changsha, Hunan 410082, China.

^b Faculty of Materials Science and Energy Engineering, Shenzhen University of Advanced Technology, Shenzhen, 518107, China.

^c Institute of Technology for Carbon Neutrality, Shenzhen Institute of Advanced Technology, Chinese Academy of Sciences, Shenzhen, 518055, China.

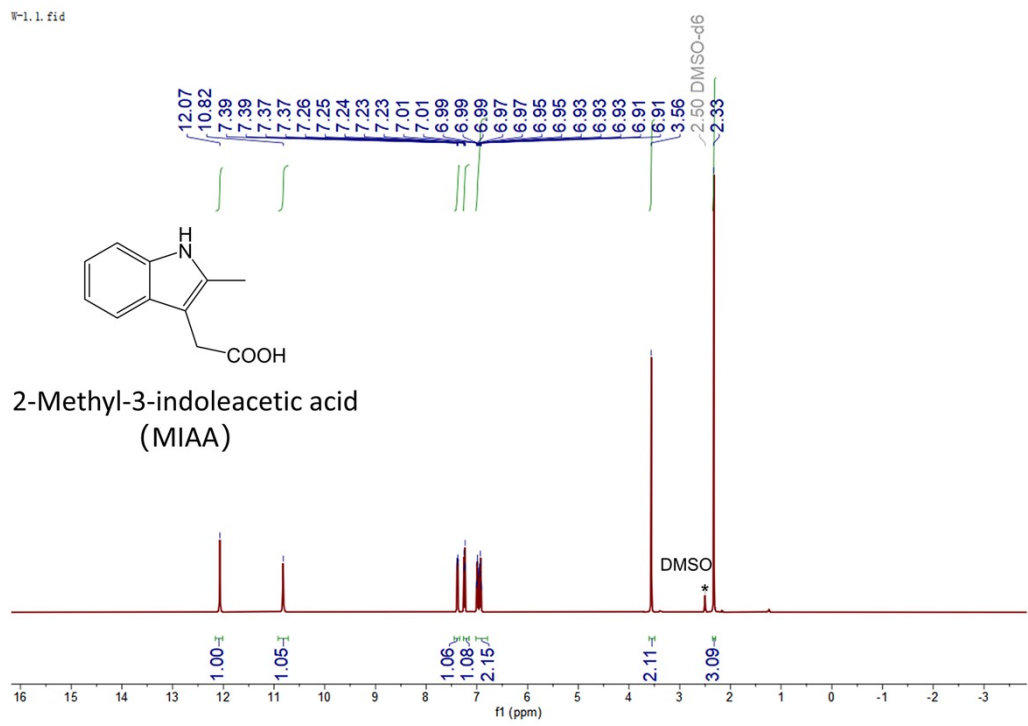


Fig. S1. Molecular structure and ^1H NMR spectra of MIAA in $\text{DMSO-}d_6$ solution.

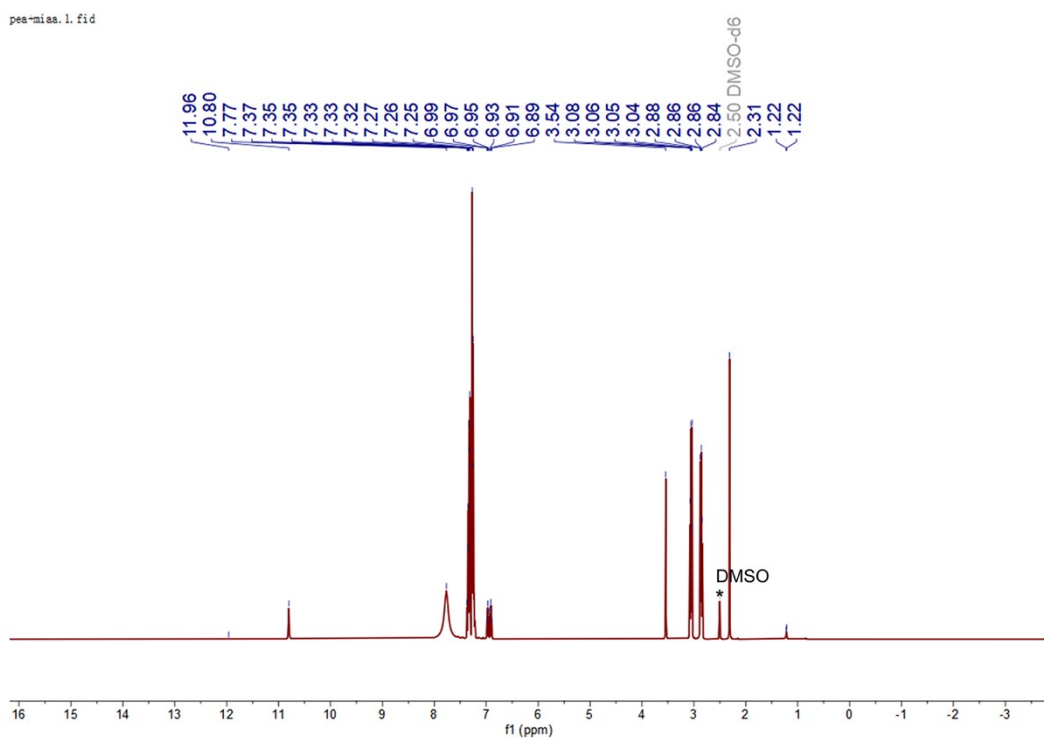


Fig. S2. ^1H NMR spectra of MIAA + PEAI in $\text{DMSO-}d_6$ solution. (Since Fig. 2 is the ^1H NMR spectrum of the mixture of two organic substances, MIAA and PEAI, no integration was performed on this hydrogen spectrum.)

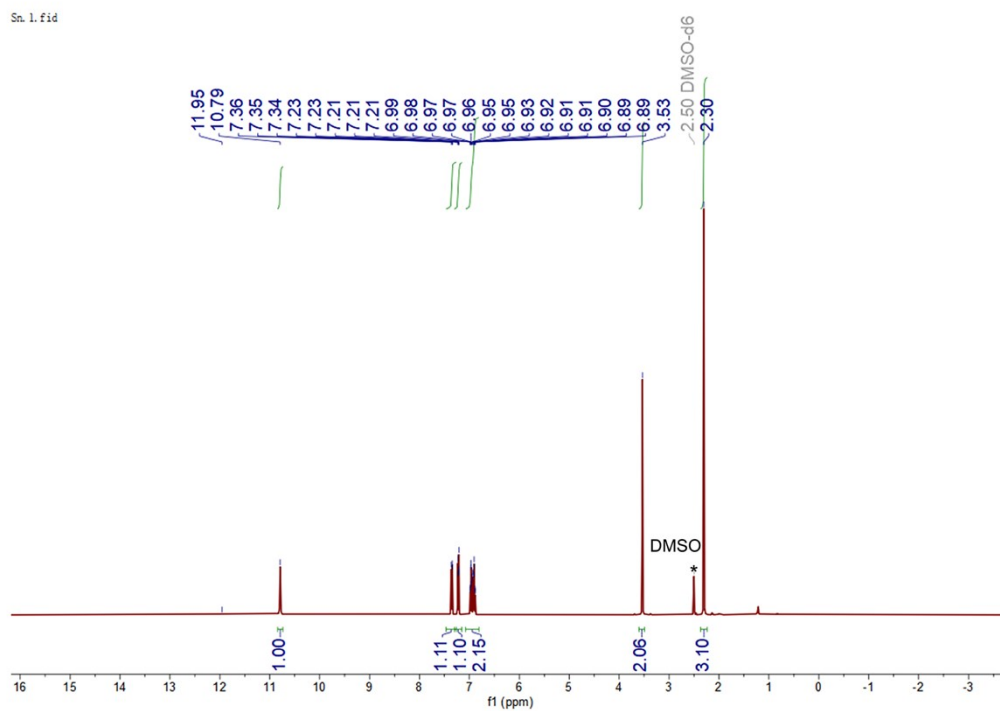


Fig. S3. ^1H NMR spectra of MIAA + SnI_2 in $\text{DMSO-}d_6$ solution.

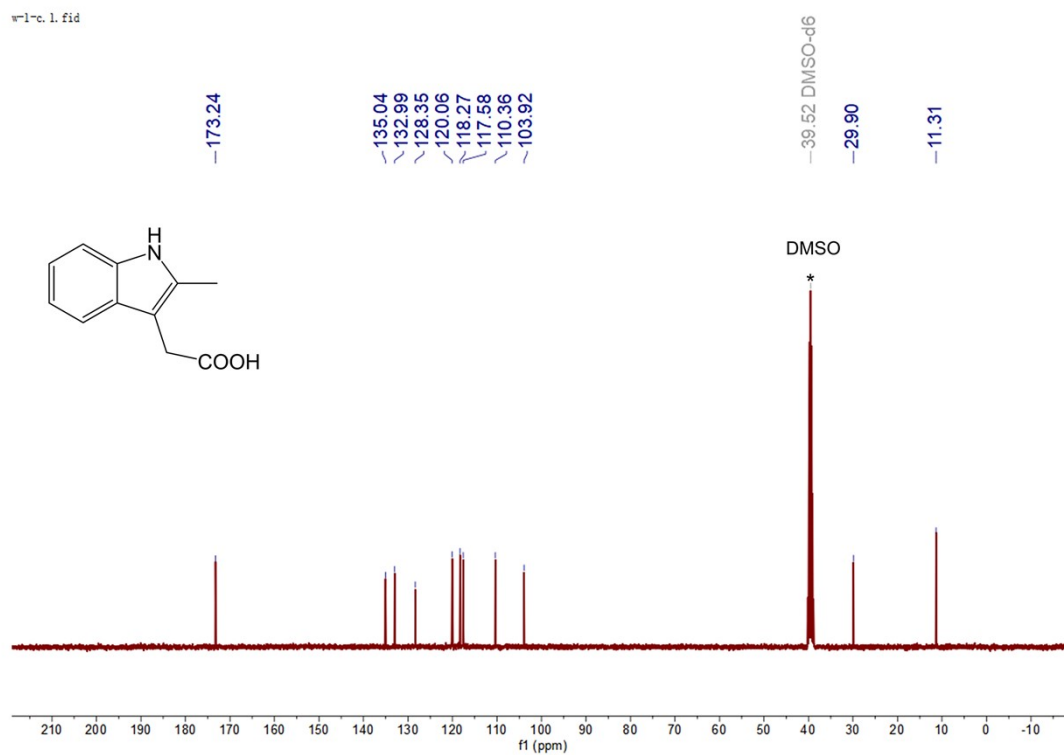


Fig. S4. ^{13}C NMR spectra of MIAA in $\text{DMSO-}d_6$ solution.

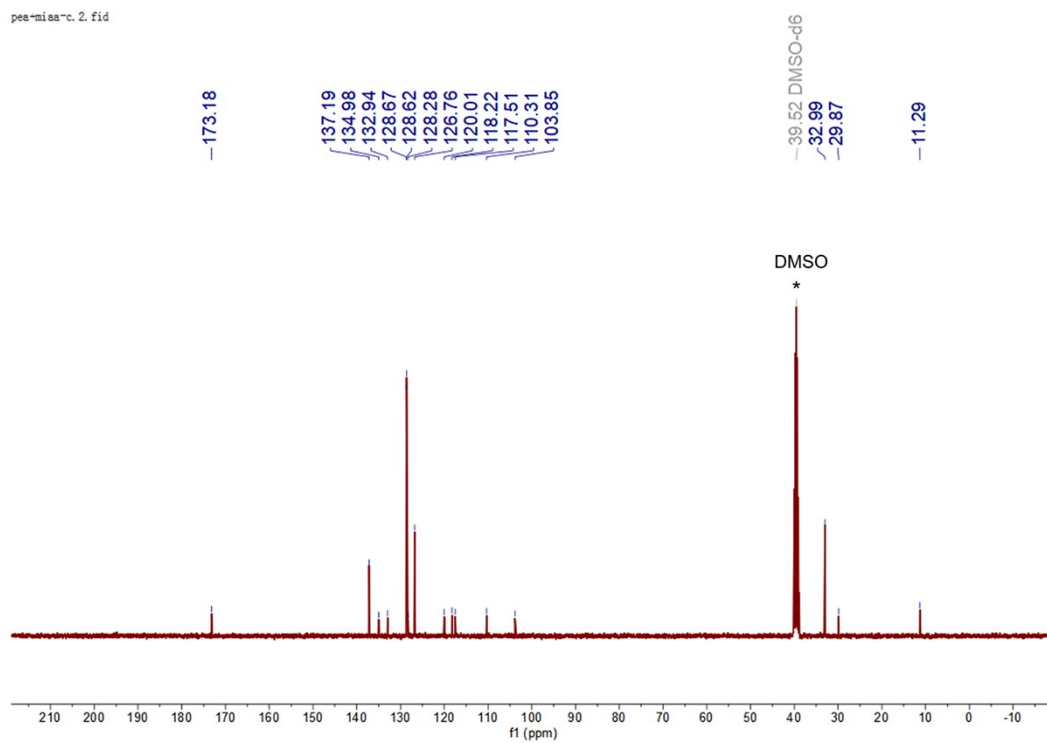


Fig. S5. ^{13}C NMR spectra of MIAA + PEAI in $\text{DMSO-}d_6$ solution.

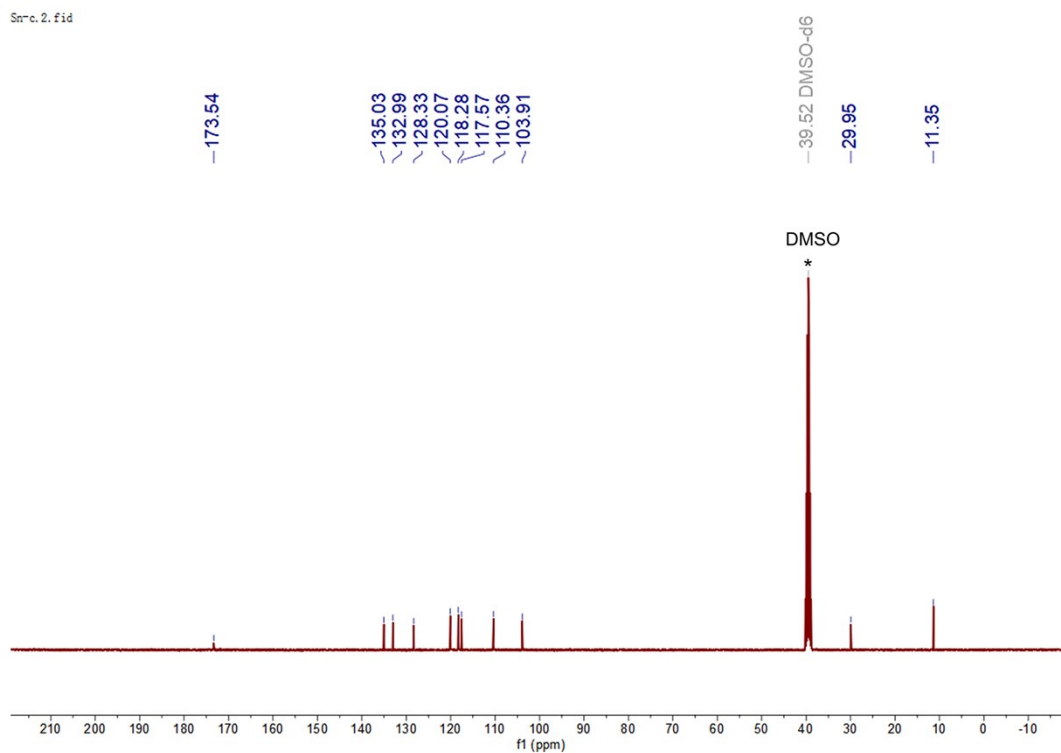


Fig. S6. ^{13}C NMR spectra of MIAA + SnI_2 in $\text{DMSO-}d_6$ solution.

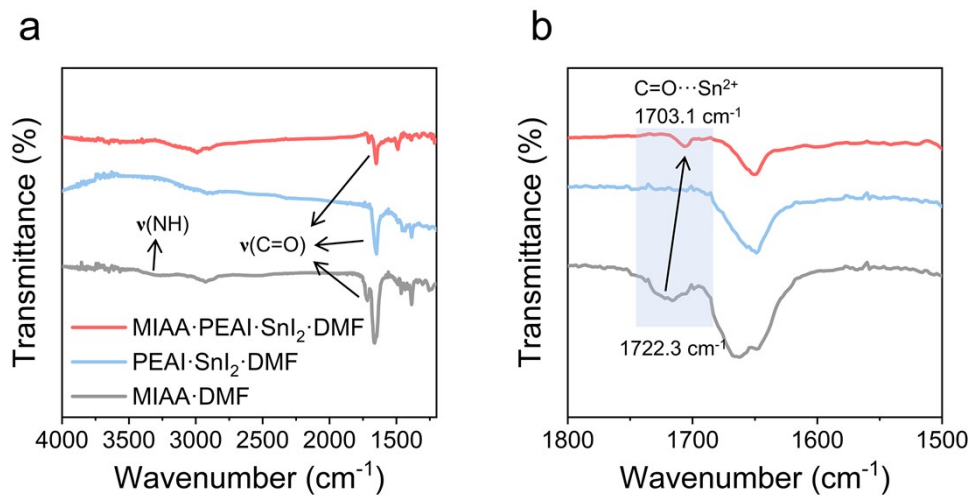


Fig. S7. (a) Full and (b) partial enlarged FTIR spectra of MIAA·DMF (powder), PEAl·SnI₂·DMF (powder), and MIAA·PEAl·SnI₂·DMF (powder).

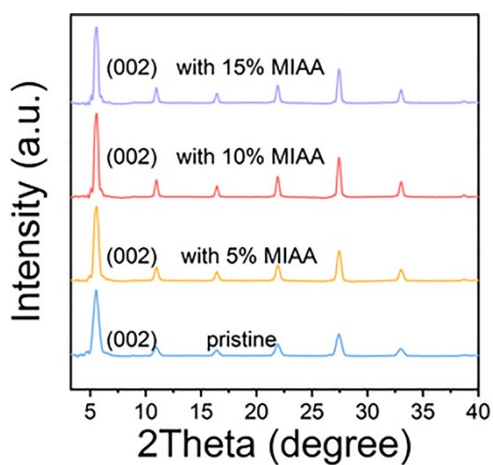


Fig. S8. XRD patterns of PEA₂SnI₄ of PEA₂SnI₄ perovskite films with different MIAA contents.

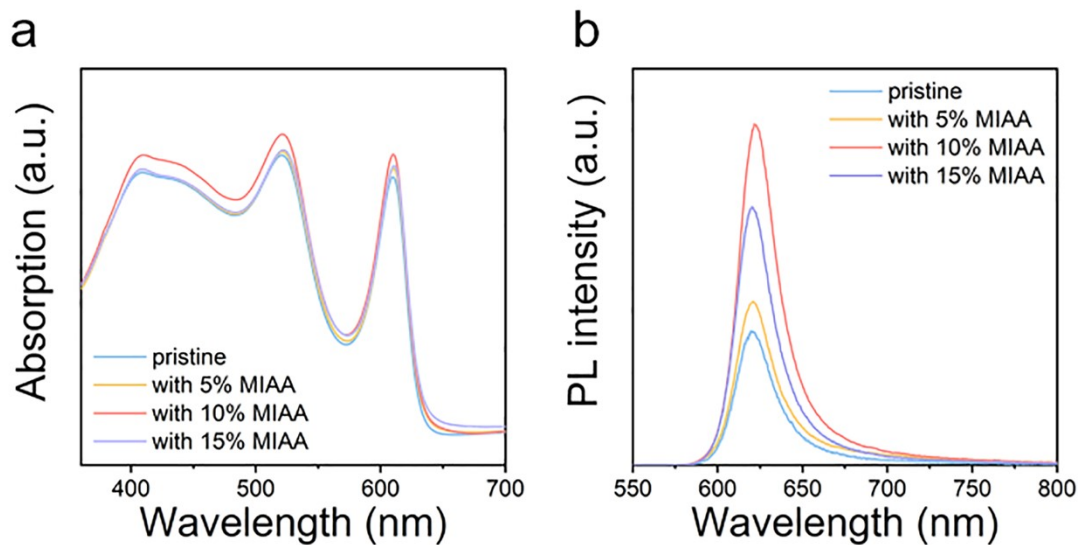


Fig. S9. (a) UV-Vis absorption spectra and (b) PL spectra of PEA₂SnI₄ perovskite films with different MIAA contents.

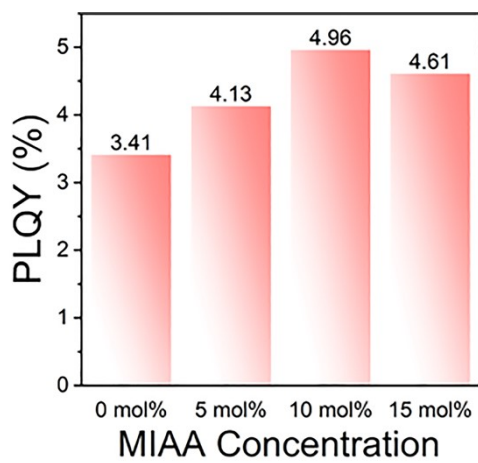


Fig. S10. PLQY of PEA₂SnI₄ perovskite films with different MIAA contents.

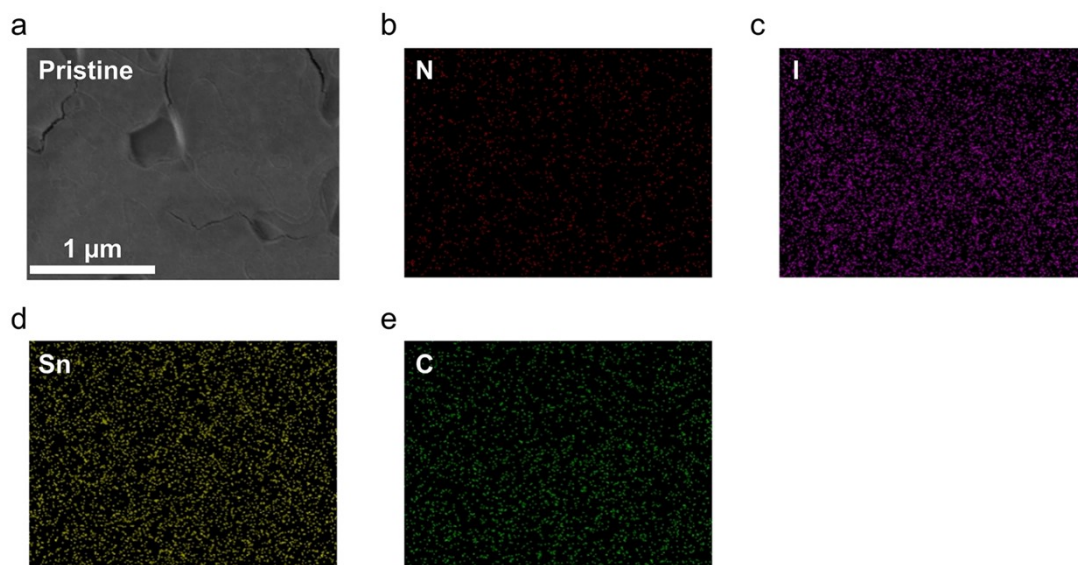


Fig. S11. (a) SEM image and (b-e) corresponding element mapping images of pristine PEA₂SnI₄ perovskite films.

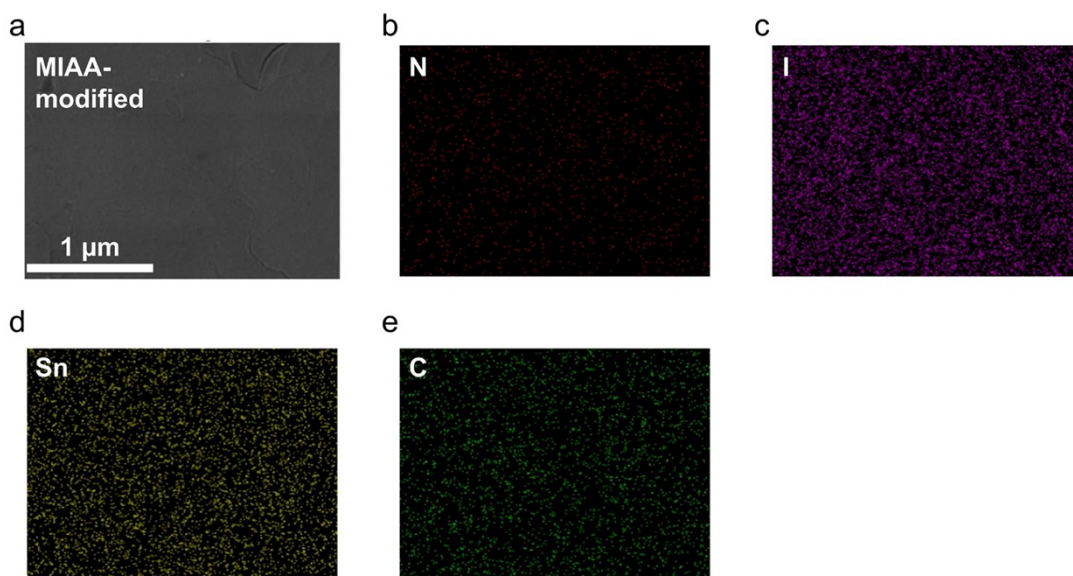


Fig. S12. (a) SEM image and (b-e) corresponding element mapping images of MIAA-modified PEA₂SnI₄ perovskite films.

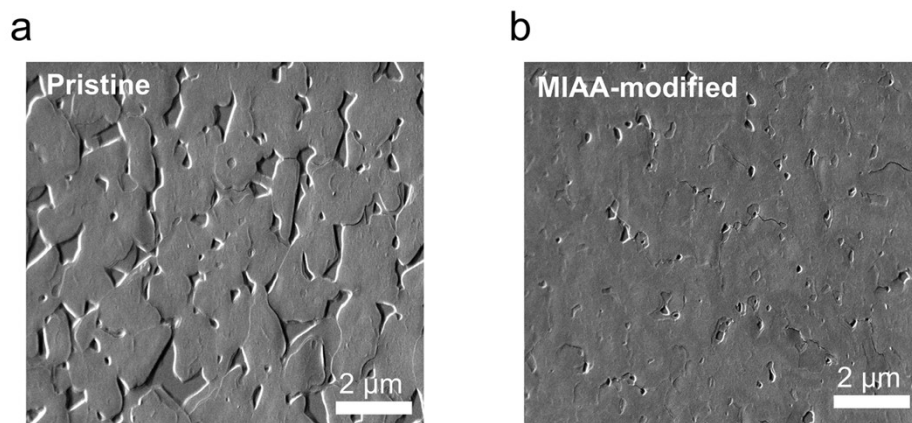


Fig. S13. SEM image of (a) pristine and (b) MIAA-modified PEA_2SnI_4 perovskite films at a 45° sample tilt angle.

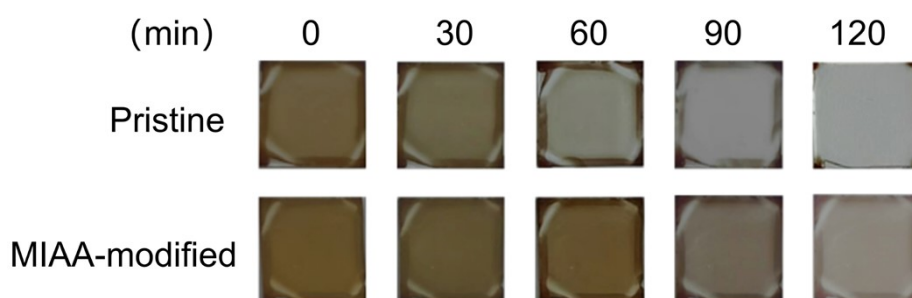


Fig. S14. Photos of pristine and MIAA-modified PEA_2SnI_4 film placing at air (20% RH, 25°C).

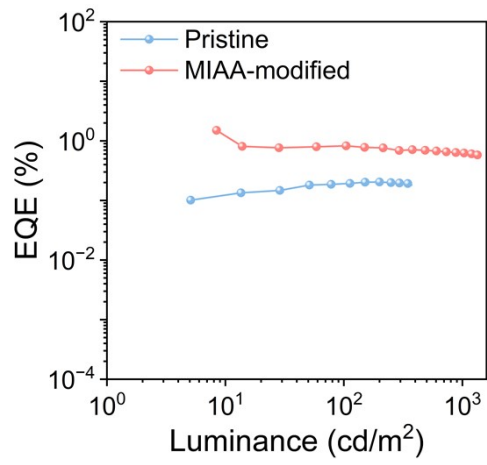


Fig. S15. EQE-Luminance curves of pristine and MIAA-modified PEA₂SnI₄ perovskite thin-film LED devices.

Table S1. TRPL fitting parameters of pristine and MIAA-modified PEA_2SnI_4 films.

Sample	τ_1 (ns)	A_1	τ_2 (ns)	A_2	τ_{avg} (ns)
Pristine	0.51	258.9	3.29	127.8	2.63
MIAA-modified	0.87	1184.3	5.87	132.8	3.02

Table S2. Summary of device performance for tin-based pure red PeLEDs with different additive.

Reference	additive	Max. Lum. (cd/m^2)	Max. EQE. (%)
<i>ACS Photonics</i> 2020, 7, 1915-1922	DSAS	132	0.7
<i>Sci. Adv.</i> 2020, 6, eabb0253	VA	~ 90	5.0
<i>Adv. Funct. Mater.</i> 2023, 33, 2301304.	DPPO-NH ₂	451	3.5
<i>Angew. Chem.</i> 2023, 135, e202312728	GSH	382	9.32
<i>Nature</i> 2023, 622, 493-498.	CA	~ 800	20.3
<i>J. Mater. Chem. C.</i> 2023, 11, 9916-9924	NHD	50	0.9
<i>J. Mater. Chem. C.</i> 2024, 12, 14368–14375	N-MTU	509	2.35
<i>Laser Photonics Rev.</i> 2025, e00727.	γ acid	371	15.5
<i>Adv. Funct. Mater.</i> 2025, 2506504	TPP	195	10.1
Our work	MIAA	1412	1.5